Fish and Shellfish Immunology 89 (2019) 326–336

Contents lists available at ScienceDirect

Fish and Shellfish Immunology

journal homepage: www.elsevier.com/locate/fsi

Full length article

*Sp*TGase plays an important role in the hemolymph clotting in mud crab (*Scylla paramamosain*)

Ngoc Tuan Tran[a,b,c,1], Weisong Wan[a,b,c,1], Tongtong Kong[a,b,c], Xixiang Tang[d], Daimeng Zhang[a,b,c], Yi Gong[a,b,c], Huaiping Zheng[a,b,c], Hongyu Ma[a,b,c], Yueling Zhang[a,b,c], Shengkang Li[a,b,c,*]

[a] Guangdong Provincial Key Laboratory of Marine Biology, Shantou University, Shantou, 515063, China
[b] Marine Biology Institute, Shantou University, Shantou, 515063, China
[c] STU-UMT Joint Shellfish Research Laboratory, Shantou University, Shantou, 515063, China
[d] Key Laboratory of Marine Biogenetic Resources, Third Institute of Oceanography, State Oceanic Administration, Xiamen, China

ARTICLE INFO

Keywords:
Scylla paramamosain
Transglutaminase
Hemolymph clotting

ABSTRACT

Transglutaminase (TGase) is important in blood coagulation, a conserved immunological defense mechanism among invertebrates. This study is the first report of the TGase in mud crab (*Scylla paramamosain*) (*Sp*TGase) with a 2304 bp ORF encoding 767 amino acids (molecular weight 85.88 kDa). *Sp*TGase is acidic, hydrophilic, stable and thermostable, containing three transglutaminase domains, one TGase/protease-like homolog domain (TGc), one integrin-binding motif (Arg^{270}, Gly^{271}, Asp^{272}) and three catalytic sites (Cys^{333}, His^{401}, Asp^{424}) within the TGc. Neither a signal peptide nor a transmembrane domain was found, and the random coil is dominant in the secondary structure of *Sp*TGase. Phylogenetic analysis revealed a close relation between *Sp*TGase to its homolog *Es*TGase 1 from Chinese mitten crab (*Eriocheir sinensis*). Expression of *Sp*TGase was investigated using qRT-PCR (1) in eight tissues from healthy mud crabs, with the highest expression in hemocytes, and (2) in response to various immune challenges (*Vibrio parahaemolyticus*, lipopolysaccharide (LPS) or Poly I:C infection), revealing a major up-regulation in hemocytes, skin, and hepatopancreas during the 96-h post injection. The recombinant *Sp*TGase showed a capacity of agglutination activities on both Gram-negative bacteria and yeast. *Sp*TGase was found to directly interact with another important blood coagulation component clip domain serine protease (*Spc*SP). Moreover, knockdown of *Sp*TGase resulted in a decreased expression of both clotting protein precursor (*Sp*preCP) and *Spc*SP and an increase of duration time in the blood coagulation. Taken together, the findings of this study suggest *Sp*TGase play an important role in the hemolymph clotting in mud crab *S. paramamosain*.

1. Introduction

Hemolymph clotting is one of the most important innate immune responses in crustaceans, which have an open circulatory system [1], forming a physical barrier to prevent hemolymph losses and microbial invasions into the hemocoel [2]. It is regulated by microbial elicitors and exhibits its roles in immunity system involving in the release of antimicrobial peptides and activation of prophenoloxidase [2–4]. In crustaceans, hemolymph clotting is mediated through plasma-clotting proteins (CPs) and hemocyte-derived transglutaminase (TGase) [5–7]. The clotting process occurred through the polymerization of CP catalyzed by a Ca^{+2}-dependent TGase that released from the hemocytes following a tissue damage or pathogen invasion [4,8–10]. TGases (Protein-glutamine: amine γ-glutamyl-transferases) are Ca^{2+}-dependent thiol enzymes that catalyze covalent crosslinks between a γ-carboxamide group of peptide-bound glutamine and a ε-amino group of peptide-bound lysine or other primary amines [10]. TGase is considered to be a prominent component in the coagulation system [11] attending to many important physiological functions, including hemolymph clotting, cell proliferation and immune response upon pathogen infections [12–14]. TGase is also known as an important immune factor in shrimp [15].

In mammals, nine TGases (TGase 1–9) were identified based on their solubility, localization, quaternary structure, functions and gene

* Corresponding author. Guangdong Provincial Key Laboratory of Marine Biology, Shantou University, Shantou, 515063, China.
E-mail address: lisk@stu.edu.cn (S. Li).
[1] These authors contributed equally to this paper.

https://doi.org/10.1016/j.fsi.2019.04.006
Received 31 December 2018; Received in revised form 17 March 2019; Accepted 3 April 2019
Available online 09 April 2019
1050-4648/

Table 1
Primers used in this study.

Primer name	Sequence (5′-3′)
cDNA cloning	
Oligo-	AAGCAGTGGTATCAACGCAGAGTACXXXXX
Long UPM	CTAATACGACTCACTATAGGGCAAGCAGTGGTATCAACGCAGAGT
Short UPM	CTAATACGACTCACTATAGGGC
NUP	AAGCAGTGGTATCAACGCAGAGT
SpTGase-3′RACE1	CTACGCCTGGATGGGAGATGACTGCT
SpTGase-3′RACE2	AACCTGTCCGGCTCCTCTTCCATTAC
SpTGase-5′RACE1	AGTTCCAAATGGAGTCGCCGAGCC
SpTGase-5′RACE2	CCACATCATCGAACTGACCGAAGGACC
SpTGase-5′RACE3	CGAACTGACCGAAGGACCAGTGCC
qRT-PCR	
SpTGase-Q F	CGGTCAGTTCGATGATGTGG
SpTGase-Q R	GGTGCCGTCAGAATAGTCCC
β-actin F	GCCCTTCCTCACGCTATCCT
β-actin R	GCGGCAGTGGTCATCTCCT
Prokaryotic expression	
SpTGase-F	CGCGGATCCTACGCAGACGACGATAAGG
SpTGase -R	CCGCTCGAGGTTGAAGGTGGCGATAAGC
RNAi	
siSpTGase-1	GATCACTAATACGACTCACTATAGGGCCAGCTGCTCACGAAGAAATT
siSpTGase-2	AATTTCTTCGTGAGCAGCTGGCCCTATAGTGAGTCGTATTAGTGATC
siSpTGase-3	AACCAGCTGCTCACGAAGAAACCCTATAGTGAGTCGTATTAGTGATC
siSpTGase-4	GATCACTAATACGACTCACTATAGGGTTTCTTCGTGAGCAGCTGGTT
SiGFP-1	GATCACTAATACGACTCACTATAGGGGGAGTTGTCCCAATTCTTGTT
SiGFP-2	AACAAGAATTGGGACAACTCCCCCTATAGTGAGTCGTATTAGTGATC
SiGFP-3	AAGGAGTTGTCCCAATTCTTGCCCTATAGTGAGTCGTATTAGTGATC
SiGFP-4	GATCACTAATACGACTCACTATAGGGCAAGAATTGGGACAACTCCTT
qRT-PCR-RNAi	
SpTGase-F	GAGGATGCCAGGGTGATAGA
SpTGase-R	GGGGTGTTACCGAAGT
SppreCP-F	GAGCCTGCCTGGGTTAA
SppreCP-R	GTCATCTAGTGAGCGGGTG
SpcSP-F	TAACTCAGTATTACGACAACGCC
SpcSP-R	TCCCTCTCCAGTAGTTACGTTCC
β-actinF	GCGGCAGTGGTCATCTCCT
β-actinR	GCCCTTCCTCACGCTATCCT

Note: Underlines indicate restriction enzyme sites.

loci on chromosomes [16,17]. These TGases are only similar in their sequence structure, but different in their substrate specificity, expression pattern, sub-cellular localization and post-translational processing [11]. TGases has been identified in various crustaceans such as horseshoe crab (*Tachypleus tridentatus*) [16,18,19], crayfish (*Pacifastacus leniusculus*) [10,13], tiger shrimp (*Penaeus monodon*) [20,21], Chinese shrimp (*Fenneropenaeus chinensis*) [22], kuruma shrimp (*Marsupenaeus japonicus*) [4], freshwater prawn (*Macrobrachium rosenbergii*) [11], Chinese mitten crab (*Eriocheir sinensis*) [9], and white shrimp (*Litopenaeus vannamei*) [15,23,24]. TGase is widely expressed in tissues at different levels, with the highest expression observed in hemocytes [11], suggesting an instant releasing into the blood coagulation system after any injury. Previous studies have documented that the up- and down-regulation of TGase in shrimp after viral and bacterial infections indicate an immune function for this gene [11,22,25]. Silencing of kuruma shrimp TGase has induced changes in gene expression, depressed the expression of crustin and lysozyme, decreased hemocyte counts and increased total bacterial counts in hemolymph [4]. Furthermore, TGase has been reported to affect the hematopoiesis, changes in cell morphology and cells spreading were observed in TGase knockdown crayfish [13]. The up-expression and decreased activity level of TGase (*Es*TGase) in the hemocytes affected by *V. parahaemolyticus* and *Staphylococcus aureus* were observed in Chinese mitten crab [9]. Silencing of *Es*TGase resulted in down-regulated expression of *Es*Crus2, *Es*LecG, and *Es*-DWD1 and caused higher bacterial counts in the hemocyte. This suggests that *Es*TGase is important in host immune response and is associated with the regulation of immunity-related genes encoding antimicrobial peptides [9].

However, so far TGase has not been reported in mud crab (*Scylla paramamosain*), an economically important crustacean species commonly consumed in Southeast Asia [26]. In this study, a full-length TGase cDNA from mud crab (*Sp*TGase) was cloned and characterized. The tissue distribution and expression profiles of *Sp*TGase after challenges with *V. parahaemolyticus*, LPS and PolyI:C were investigated. The recombinant *Sp*TGase (r*Sp*TGase) showed agglutination activities towards both Gram-negative bacteria and yeast and could interact with clip domain serine protease (*Sp*cSP), another important component during blood coagulation in mud crab. Furthermore, the RNAi experiments were conducted to investigate the relationship between *Sp*TGase and clotting protein precursor (*Sp*preCP) or *Sp*cSP expression as well as the hemolymph clotting capacity. The results of this study provide an insight into the structure and function of *Sp*TGase in the hemolymph clotting in mud crab.

2. Materials and methods

2.1. Experimental animals, immune challenges and sample collections

A total of 64 healthy mud crabs (approximately 100 g each) were purchased from a culture farm in Shantou (Guangdong, China). The mud crabs were acclimatized in tanks at the laboratory conditions (salinity of 8‰ and water temperature of 25 °C) for one week before the further experiments.

The immune challenges included four groups, corresponding to either injection with a negative control (sterile physiological saline), or with a concentration of *V. parahaemolyticus* (1×10^7 colony-forming units (*cfu*) mL^{-1}), lipopolysaccharide (LPS) (0.5 mg mL^{-1}), or Poly I:C (1 mg mL^{-1}). Each group was maintained in a separate tank. Mud crabs

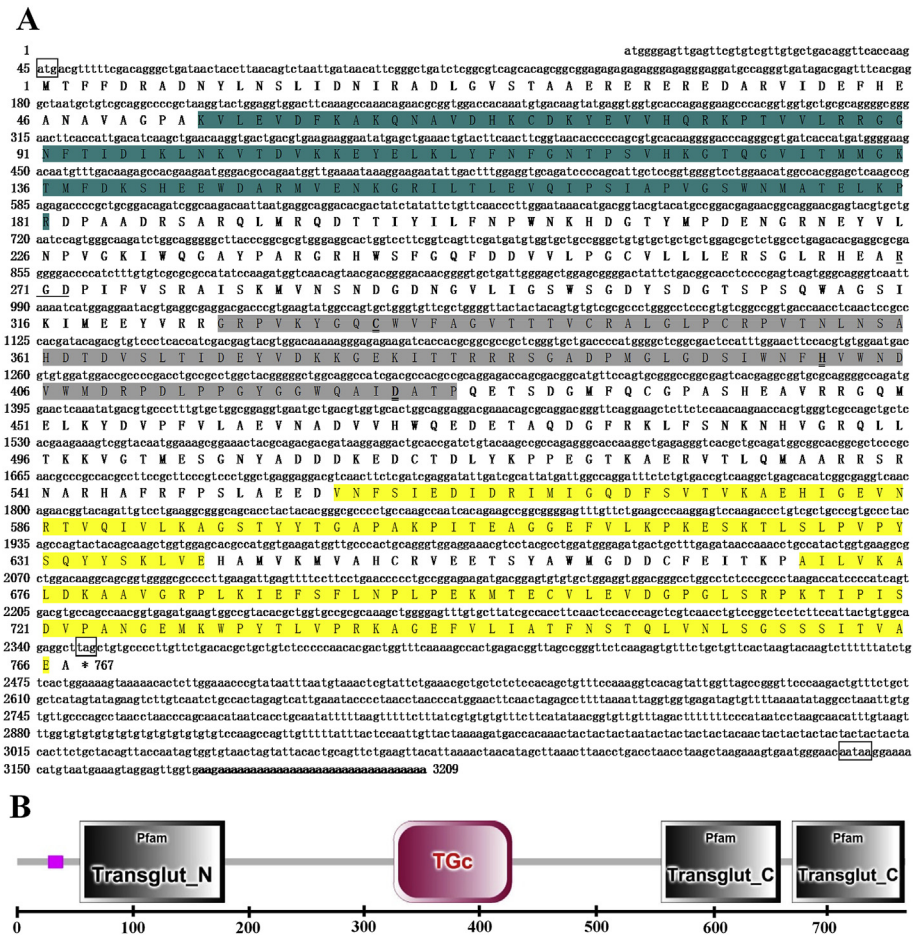

Fig. 1. Sequences and domain topology of *Sp*TGase. (A) The nucleotide (upper row) and deduced amino acid (lower row) sequence are shown and numbered on the left. The start codon (atg), stop codon (tag) and polyadenylation signal (aataa) are boxed. The integrin-binding motif (RGD) is underlined and the catalytic triad is bolded and double-underlined. The three transglut domains are highlighted in cyan and yellow, and the TGase/protease-like homolog domain (TGc) is highlighted in gray. (B) The domain topology of *Sp*TGase protein, generated by Simple Molecular Architecture Research Tool (SMART), showing the transglut and TGc domains. (For interpretation of the references to color in this figure legend, the reader is referred to the Web version of this article.)

were given an injection of a volume of 200 μL of saline or suspension of bacteria, LPS, or Poly I:C. At 0, 6, 12, 24, 48 and 96 h post-injection (hpi), hemolymph from each anesthetized crab was withdrawn using a 1-mL disposable syringe, collected into tubes that preloaded with an equal volume (750 μL) of ice-cold anticoagulant solution (1.32% sodium citrate, 0.48% citricacid,1.47% glucose), and immediately centrifuged at 800 × *g* for 20 min at 4 °C to separate the hemocytes, which were then used for RNA extraction using TRIzol® Reagent (Ambion, USA). Other tissues (including heart, brain, skin, gills, muscles, hepatopancreas, and intestine) from three mud crabs were collected, immediately preserved in liquid nitrogen, and stored at −80 °C prior to RNA extraction.

2.2. cDNA cloning, sequencing and bioinformatics analysis

Total RNA extracted from hemocytes were incubated at 37 °C for 30 min with 10 units of DNase I (Takara, Dalian, China) to remove genomic DNA contamination. The quality and quantity of RNA were evaluated by electrophoresis in 1.0% agarose gel and Nanodrop® ND-2000 spectrophotometer (Thermo Fisher Scientific, USA). The first-strand cDNA was synthesized using the M-MLV First-Strand cDNA Synthesis Kit (Invitrogen, USA) following the manufacturer's instructions.

The partial cDNA sequence of *Sp*TGase was obtained from our previous transcriptomic data. The complete *Sp*TGase cDNA was amplified using the SMARTer™ RACE cDNA Amplification Kit (Clontech, USA) *via* the touchdown and nested PCR strategy [26,27]. Amplification primer pairs for *Sp*TGase are shown in Table 1. PCR was carried out using 25 μL of PreMix LA Taq (TaKaRa, Dalian, China), 16.5 μL of ultra-pure water, 1 μL of *Sp*TGase-3′RACE1 or *Sp*TGase-5′RACE1 primer, 5 μL of UPM, and 2.5 μL of cDNA template in a total volume of 50 μL. The touch-down PCR was programmed as follows: 94 °C for 3 min; 5 cycles at 94 °C for 30 s, 72 °C for 2 min; 5 cycles at 94 °C for 30 s, 68 °C for 30 s, 72 °C for 2 min; and 27 cycles of 94 °C for 30 s, 64 °C for 30 s, 72 °C for 2 min; and a final extension at 72 °C for 10 min. The product of touch-down PCR was used as templates for the subsequent nested PCR. The nested PCR was also performed in a 50-μL reaction volume containing 25 μL of PreMix LA Taq (TaKaRa, Dalian, China), 20.5 μL of ultra-pure water, 1 μL of *Sp*TGase-3′RACE2 or *Sp*TGase-5′RACE2, *Sp*TGase-5′RACE3 primer, 1 μL of NUP primer, and 2.5 μL of the template. The nested PCR was performed as follows: 94 °C for 3 min, followed by 35 cycles at 94 °C for 30 s, 64 °C for 30 s, 72 °C for 2 min; and a final extension at 72 °C for 10 min. The expected DNA fragment was retrieved using the SanPrep Column DNA Gel Extraction Kit (Sangon, Shanghai, China). The purified DNA fragment was inserted into pMD®19-T vector (TaKaRa, Dalian, China) and then transformed into *Escherichia coli* DH5α. Positive clones were identified by PCR screening with M13 R&F primers and then sequenced by a commercial company (BGI, Shenzhen, China).

The full-length sequence of *Sp*TGase was identified by BLAST homology search in the GenBank database (http://blast.ncbi.nlm.nih.gov/Blast). The open reading frame (ORF) and deduced amino acid sequence were inferred using ORF Finder (http://www.ncbi.nlm.nih.gov/gorf/orfig.cgi). The homologous conserved domains and signal peptide were inferred using SMART (http://smart.embl-heidelberg.de/), signal peptide and transmembrane helices using SignalP server (http://www.cbs.dtu.dk/services/SignalIP/), multiple protein sequences alignments using the Clustal Omega (http://www.ebi.ac.uk/Tools/msa/clustalo/), and coloring using DNAman version 6.0. The phylogenetic analysis was conducted with MEGA 6.0.6 using Neighbor-

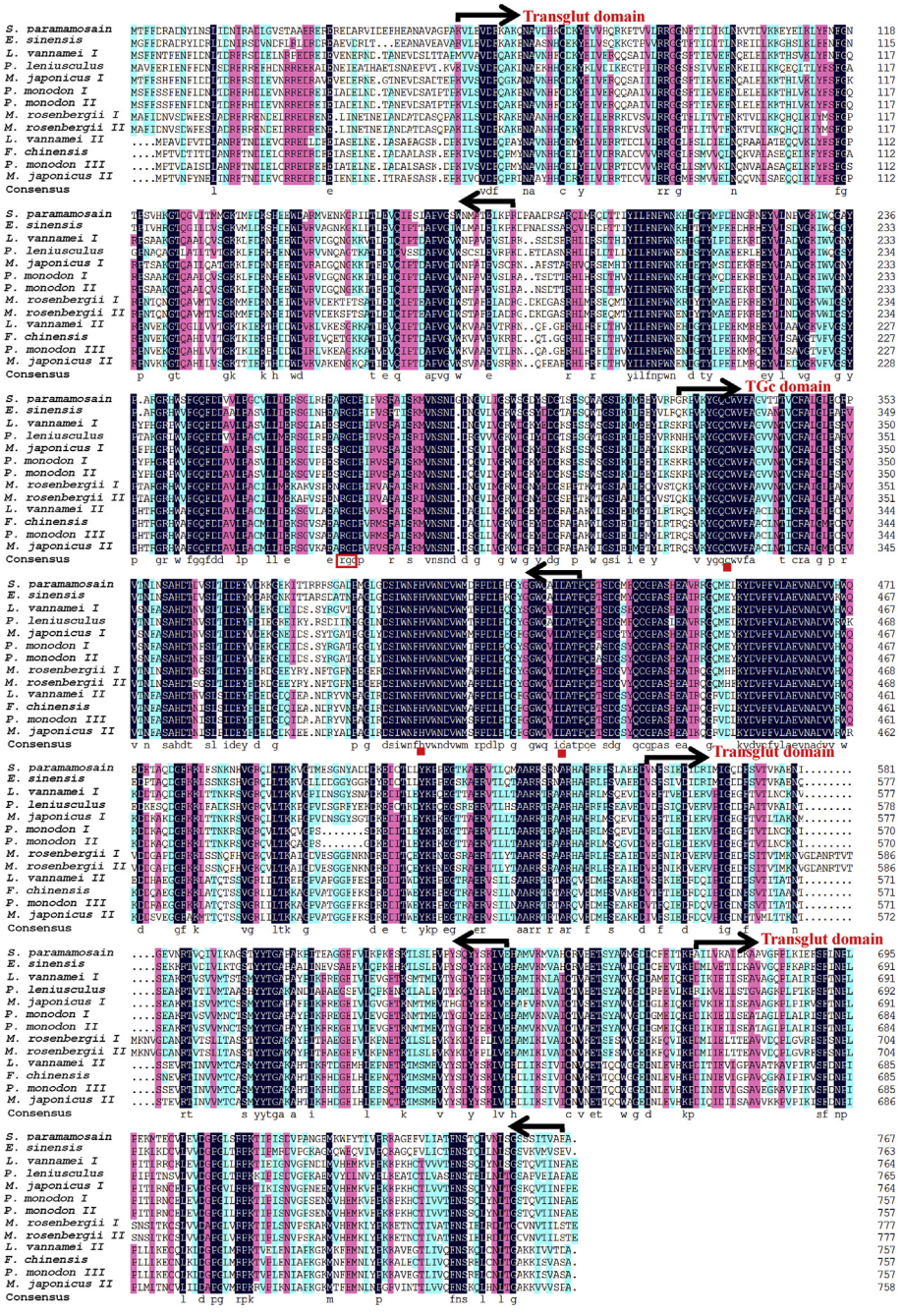

Fig. 2. Multiple amino acid sequence alignment of *Sp*TGase and other crustacean homologs. *Eriocheir sinensis (EsTGase, ADF87938), Litopenaeus vannamei (LvTGaseI, ABX83902; LvTGaseII, ABN13875), Pacifastacus leniusculus (PlTGase, AAK69205), Marsupenaeus japonicus (MjTGaseI, BAD36808; MjTGaseII, ABD92928), Penaeus monodon (PmTGaseI, AAV49005; PmTGaseII, AAO33455, PmTGaseIII, AAL78166), Macrobrachium rosenbergii (MrTGaseI, CCQ25772; MrTGaseII, ADX99580), Fenneropenaeus chinensis (FcTGase, ABC33914) using the Clustal Omega program and further colored by DNAman. Conserved amino acids are shaded, whereas identical (black color) and similar (red (> 75%) and aqua (> 50%)) residues are indicated. The catalytic triad sites are indicated by the red square dots. The putative integrin-binding motif (KGD) is boxed in red. Arrows indicate the transglut and TGase/protease-like homolog domains. (For interpretation of the references to color in this figure legend, the reader is referred to the Web version of this article.)*

Joining method (https://www.megasoftware.net/). The physicochemical properties of the protein were computed using Expasy's ProtParam server (http://web.expasy.org/protparam/). SOSUI server (http://harrier.nagahama-i-bio.ac.jp/sosui/) was used to identify the type of protein. CYS_REC server (http://linux1.softberry.com/) was applied to predict the presence of disulfide bonds and their bonding patterns. Three-dimensional (3-D) structure of *Sp*TGase was predicted using SWISS-MODEL (http://swissmodel.expasy.org/). Stereochemical quality and accuracy of the predicted models were analyzed using PROCHECK's Ramachandran plot analysis, ERRAT, PROVE, Verify3D (all four available from the SAVES server at http://servicesn.mbi.ucla.edu/SAVES/), ProQ [28] and ProSA [29,30]. The structural similarity and functional annotation were predicted using COFACTOR web server (https://zhanglab.ccmb.med.umich.edu/COFACTOR/).

2.3. Quantitative RT-PCR analysis

Total RNA was extracted from tissues followed by cDNA synthesis using the *Transcript*® One-Step gDNA Removal and cDNA Synthesis SuperMix (Transgen Biotech, China) following the manufacturer's instructions. The quantitative RT-PCR (qRT-PCR) analysis was carried out using the *TransStart*® Tip Green qRCR SuperMix (Transgen Biotech, China) on a LightCycler® 480 (Roche, USA). The reaction volume of 20 mL contained 10 μL of 2 × PCR Mix, 1 μL of 10 mM each of the forward and reverse primer (Table 1), 7 μL of ultra-pure water, and 2 μL of cDNA template. β-actin was used as the reference gene (Table 1). Thermal conditions were as follows: denaturation at 95 °C for 30 s, and 40 cycles of 95 °C for 5 s, 60 °C for 20 s, followed by a melting curve analysis of 95 °C for 1 s, 65 °C for 15 s. All reactions were performed in triplicate and the PCR products were checked by electrophoresis in 3.0% agarose gel and visualized under ultraviolet light. The PCR data

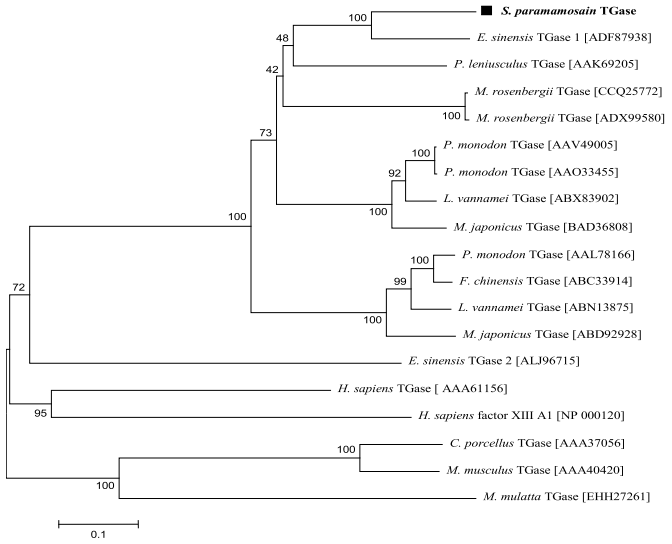

Fig. 3. Neighbor-Joining phylogenetic tree of *Sp*TGase with other homologs. The numbers at the branches indicate bootstrap values (1000 replications). The bar (0.1) indicates the genetic distance. *Sp*TGase is bolded and marked by a black square dot.

were analyzed using the LightCycler 480 software (Roche, USA). The relative transcript level was determined using the $2^{-\triangle\triangle Ct}$ method [31] based on a normalization to the reference gene. All data were expressed as means ± SE. Data were subjected to one-way ANOVA analysis; $P < 0.05$ and $P < 0.01$ were considered statistically significant and extremely significant, respectively.

2.4. Prokaryotic expression and purification of recombinant SpTGase

The *Sp*TGase was amplified with the specific primers (*Sp*TGase-F and *Sp*TGase-R, Table 1), followed by digestion of the product with *Bam*H I and *Xho* I, inserted into the expression vector pET32a cut with the same restriction enzymes and then transformed into the competent *Rosetta* host cells (Novagen, Inc., Germany). Positive clones were identified either by PCR with the primers S.tag and T7ter or by sequencing. The positive transformants were grown in 300 mL of LA medium (LB medium added 100 μg mL^{-1} ampicillin) at 37 °C, 180 rpm and induced with 0.1 mM isopropyl β-D-1-thiogalactopyranoside (IPTG) at 20 °C, 140 rpm until the OD_{600} value reached 0.6. The bacteria were collected by centrifugation at 5500 rpm for 10 min and resuspended in 20 mL of Tris-HCl buffer (20 mM Tris-HCl, pH 8.0, 0.1 M NaCl) containing 0.1% TritonX-100. The collected bacteria were lysed using ultrasonication. The soluble fraction was purified using *ProteinIso*™ GST resin (Transgen Biotech, China) following the manufacturer's instructions. The purified protein was evaluated using 10% SDS polyacrylamide gel electrophoresis (SDS-PAGE) and visualized using a Coomassie brilliant blue R250. The concentrations of the r*Sp*TGase protein were quantified by the BCA Protein Assay Kit (Tiangen Biotech, Beijing).

2.5. Microbial agglutination assay

The microbial agglutinating assay was carried out according to the previously published method Okino, Kawabata [32]. Briefly, 4, 6-diamidino-2-phenylindole (DAPI) stained *Vibrio alginolyticus*, *V. parahaemolyticus*, *Aeromonas hydrophila*, and *Saccharomyces cerevisiae* were suspended in TBS-Ca^{2+} buffer (50 mM Tris-HCl, 100 mM NaCl, 50 mM $CaCl_2$, pH 7.4) at 2×10^9 cfu mL^{-1}. The suspension of bacterial or

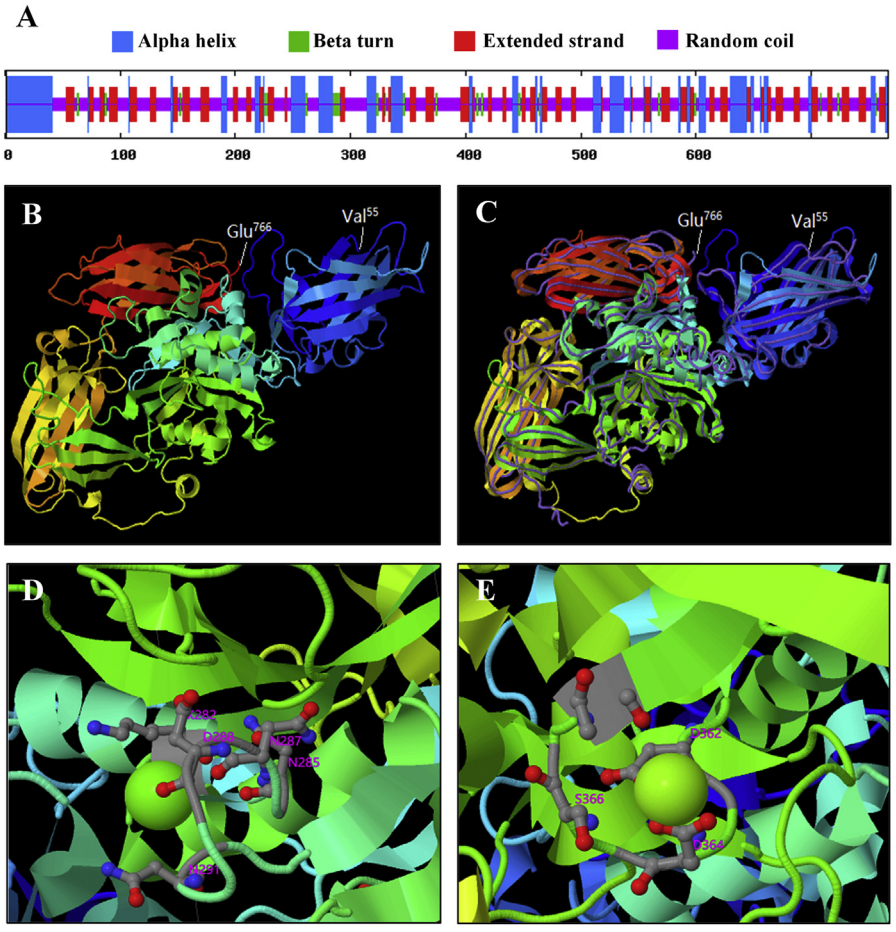

Fig. 4. Structure of the *Sp*TGase. (A) Secondary structure model of *Sp*TGase, rendered using self-optimized prediction method by alignment (SOPMA) server. (B) Three-dimensional homology model rendered by the SWISS-MODEL program. (C) Structural alignment of *Sp*TGase (shown in cartoon) and human TGase structural analog (PDB ID: 1l9m) (backbone trace) rendered by COFACTOR server. (D) The Ca^{2+}-binding sites (Lys^{282}, Asn^{285}, Asn^{287}, Asp^{288}, and Asn^{291}) and (E) the Mg^{2+}-binding sites (Asp^{362}, Asp^{364}, Ser^{366}, and Thr^{368}) predicted by COFACTOR server.

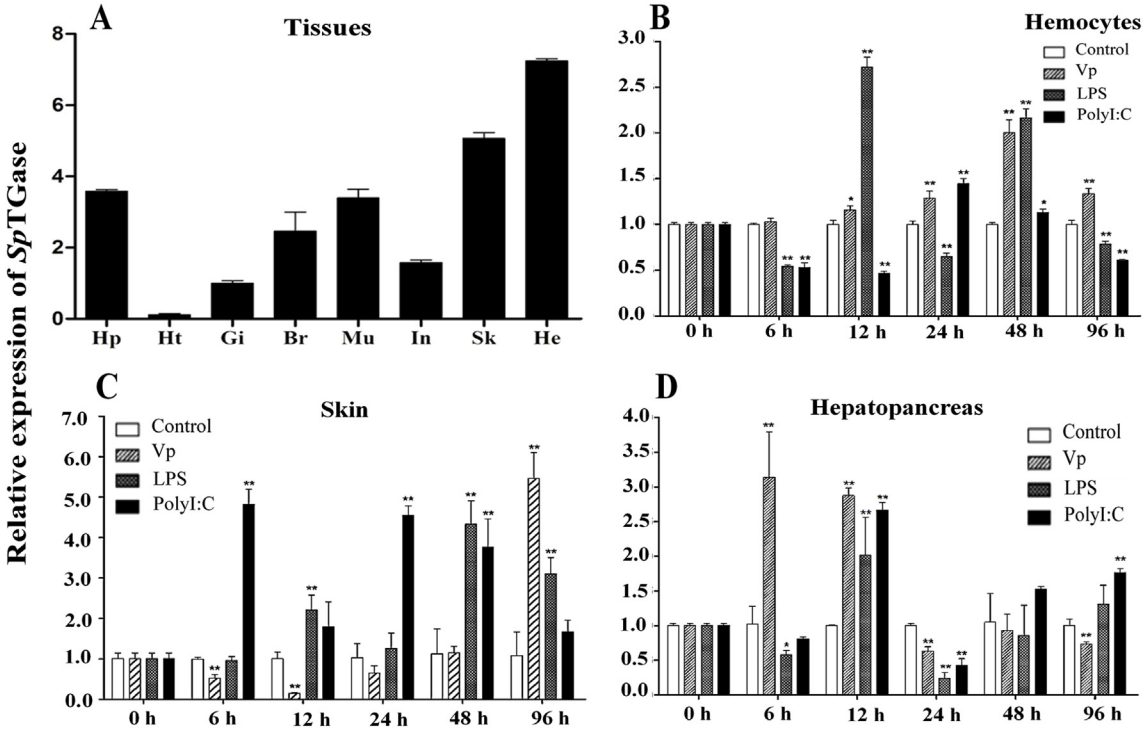

Fig. 5. Expression profiles of *Sp*TGase, inferred *via* qRT-PCR, in hepatopancreas (Hp), heart (Ht), gills (Gi), brain (Br), muscles (Mu), intestine (In), skin (Sk), and hemocytes (He) of healthy mud crabs (A) and hemocytes, skin, and hepatopancreas of mud crab at 0, 6, 12, 24, 48, and 96 h post-injection with *V. parahaemolyticus* (Vp), lipopolysaccharide (LPS) and PolyI:C (B, C, and D, respectively). Data were normalized to the β-actin as a reference gene. Each histogram represents the mean ± SE of three replicates. Statistically significant differences from the control group are marked as * $P < 0.05$ and ** $P < 0.01$.

yeast (20 mL) was added to 20 mL of r*Sp*TGase (1.8 μg mL^{-1}) dissolved in TBS-Ca^{2+} buffer (set as treatment groups), or rTrx protein (1.8 μg mL^{-1}) dissolved in the same buffer (set as a negative control). The mixtures were incubated at room temperature for 2 h and the cells were then observed by fluorescence microscopy (Leica). To determine whether the agglutination of the microbes required Ca^{2+}, DAPI-labeled *V. alginolyticus*, *V. parahaemolyticus*, *A. hydrophila* and *S. cerevisiae* were incubated with *rSp*TGase (~3.6 μg mL^{-1}) in TBS-Ca^{2+}-EDTA buffer (TBS-Ca buffer containing 50 mM EDTA, pH 7.4) under the same conditions described above.

2.6. Far-western blot assay

To evaluate the interaction between *Sp*TGase and *Spc*SP (a hemolymph clotting component in mud crab) [33], a far-western blot assay was performed. The proteins were separated by 12% SDS-PAGE and transferred to a polyvinylidene fluoride (PVDF) membrane (Millipore, USA). The membrane was incubated in Tris buffer containing 5% fat-free milk at room temperature for 1–2 h, and then washed three times with TTBS (containing 0.05% (v/v) Tween 20). The membrane was incubated with rabbit anti-*Spc*SP antibody at 37 °C for 1 h, washed three times with TTBS, and then incubated with goat anti-rabbit IgG HRP-conjugate antibody for 1 h. After washing three times with TTBS, the protein was visualized using an Enhanced HRP-DAB Chromogenic Substrate Kit (Tiangen, German) according to the manufacturer's instructions.

2.7. RNA interference

Small interfering RNA duplexes (siRNA) targeting *Sp*TGase (siRTGaseR: 5′- GATCACTAATACGACTCACTATAGGGCCAGCTGCTCA CGAAGAAATT-3′) and random siRNA (siGFPF: 5′-UUCUCCGAACGUG UCACGUTT-3′) used as negative control were chemically synthesized by Gene-Pharma (Shanghai, China). All siRNAs were diluted to a final concentration of 125 μg mL^{-1} with DEPC-water. RNA oligonucleotides used in this study are in Table 1. To determine the RNA interference efficiency, laboratory-acclimatized mud crabs (n = 30, approximately 50 g each) were injected with 200 μL of si*Sp*TGase (50 μg $crab^{-1}$) (set as an experimental group) or random siRNA (set as controls) at the base of the fourth leg. At 6, 12, and 24 hpi, hemocytes from three mud crabs were randomly collected from each group. The hemocytes were used for further processing, including RNA extraction, cDNA synthesis, and qRT-PCR assay and analysis.

2.8. Hemolymph clotting

A total of 50 mud crabs (approximately 50 g each) were divided into two groups (25 mud crabs each), with one group injected with 200 μL siGFP (50 μg $crab^{-1}$) (negative control) and another with the same volume of si*Sp*TGase (50 μg $crab^{-1}$). At 6, 12 and 24 h post siRNA treatment, four mud crabs (per group) were randomly sampled; hemolymph (200 μL) was drawn out from the fourth leg of each crab using a 1-mL syringe. The duration time of hemolymph coagulation was observed and recorded. All data were expressed as means ± SE. Data were analyzed using *t*-test and one-way analysis of variance (ANOVA) using OriginPro version 7.0.

3. Results

3.1. Sequence analyses, homology analysis and phylogenetic tree construction

The full *Sp*TGase sequence (3209 bp) (deposited in the NCBI GenBank database under the accession number LN994608) contains a 44 bp 5′ untranslated region (UTR), an 2304 bp ORF encoding 767 amino acids, and an 861 bp 3' UTR including a stop codon (TAG), a putative polyadenylation consensus signals (AATAA) and a poly (A) tail (Fig. 1). The mature protein has a molecular weight of 85.88 kDa with a

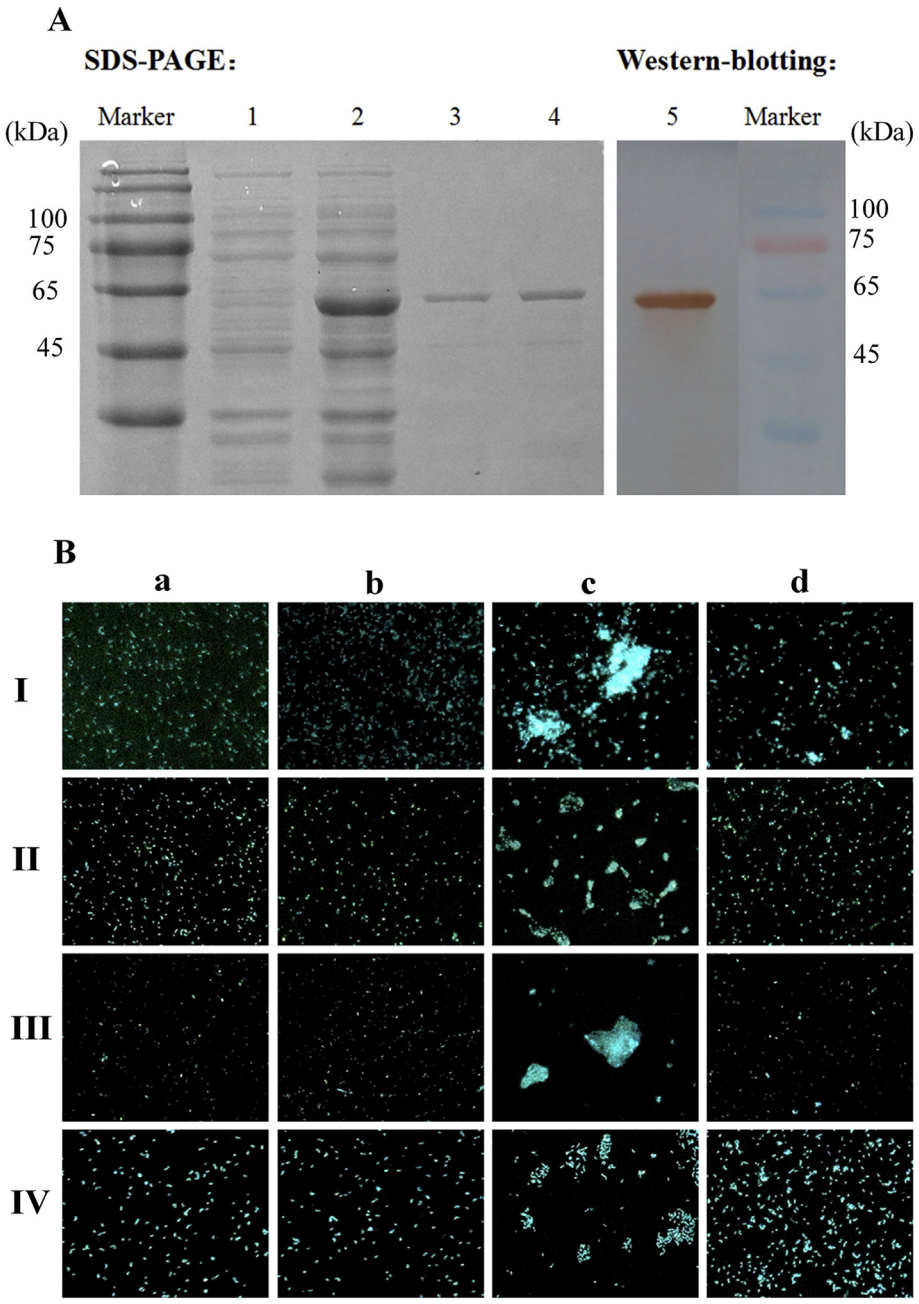

Fig. 6. The purification and agglutination activity of r*Sp*TGase. (A) SDS-PAGE and Western blot analysis of r*Sp*TGase in *Rosetta*. Lane 1, total proteins of *Rosetta* with pGEX4T-1-*Sp*TGase, without induction; lane 2, total proteins of *Rosetta* with pGEX4T-1-*Sp*TGase, induction with IPTG; lane 3 and 4, purified r*Sp*TGase *via* GST resin chromatography; lane 5, Western blot of purified r*Sp*TGase use Anti-GST mouse monoclonal antibody; Marker, 180 kDa of color pre-stained protein marker. (B) Agglutination activity of r*Sp*TGase. *V. alginolyticus* (I), *V. parahaemolyticus* (II), *A. hydrophila* (III) and *S. cerevisiae* (IV) were incubated with (a) TBS-Ca buffer, (b) GST protein, (c) r*Sp*TGase, (d) r*Sp*TGase plus EDTA. Magnification: 15 × 40. (For interpretation of the references to color in this figure legend, the reader is referred to the Web version of this article.)

theoretical isoelectric point of 5.95, which is constructed by a predominance of valine (8.5%), alanine and glycine (both share 7.4%). The number of negative (Asp + Glu) and positive (Arg + Lys) residues is 106 and 95, respectively. The extinction coefficient measured at 280 nm is 117,395 $M^{-1}\,cm^{-1}$ (assuming all pairs of cysteine residues form cysteines) and 116,770 $M^{-1}\,cm^{-1}$ (assuming all cysteine residues are reduced). The instability index, aliphatic index and grand average hydropathicity values of *Sp*TGase is 35.74, 75.23 and −0.459, respectively. *Sp*TGase is a soluble protein and 10 cysteine residues found in its sequence, with the most probable pattern of pairs of Cys^{344}-Cys^{702} and Cys^{351}-Cys^{515}. The analysis showed that the *Sp*TGase contains an integrin-binding motif (RGD). Neither a signal peptide nor a transmembrane domain was found in *Sp*TGase sequence. The protein comprises a conserved Transglutaminase-like homologous (TGc) domain (at positions Gly^{325}-Pro^{427}) and there are three catalytic sites (Cys^{333}, His^{401} and Asp^{424}) were found within the TGc domain.

*Sp*TGase had the highest sequence similarity with the TGases from *E. sinensis* (accession number ADF87938) (74%) and other invertebrates (> 52%), particularly *L. vannamei* (ABX83902) and *P. leniusculus* (AAK69205) (both share 60%), *P. monodon* (AAV49005 and AAO33455) (59%), *M. rosenbergii* (CCQ25772 and ADX99580) (56%), *F. chinensis* (ABC33914) (54%), and *M. japonicus* (ABD92928) (52%) (Fig. 2). Both integrin-binding motif and catalytic triads were fully conserved. An *N*-J phylogenetic tree, constructed using homologous amino acid sequences from multiple species, revealed that *Sp*TGase formed a clade with *E. sinensis* (ADF87938), which are grouped together with TGases from other crustaceans (Fig. 3).

3.2. Structural and functional predictions

The structure analysis showed that random coil (44.46%) was predominant among the secondary structure elements, followed by extended strand (28.86%), alpha helix (23.47%) and beta turn (5.22%). Other elements such as 3_{10}helix, pi helix, beta bridge, bend region, and

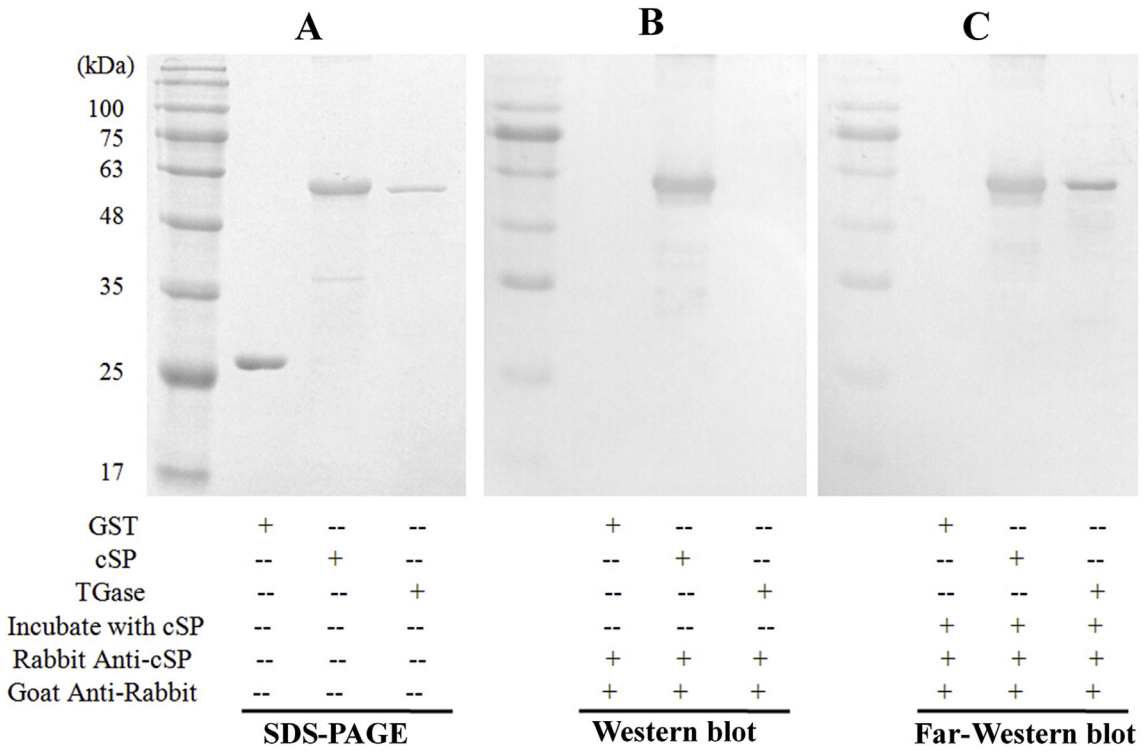

Fig. 7. The interaction between *Sp*TGase and *Spc*SP. (A) The SDS-PAGE analysis of GST, *Spc*SP and *Sp*TGase, which all used as controls. (B) GST, *Spc*SP, and *Sp*TGase were analyzed using Western blot analysis. (C) GST, *Spc*SP, and *Sp*TGase were analyzed using far-Western blot.

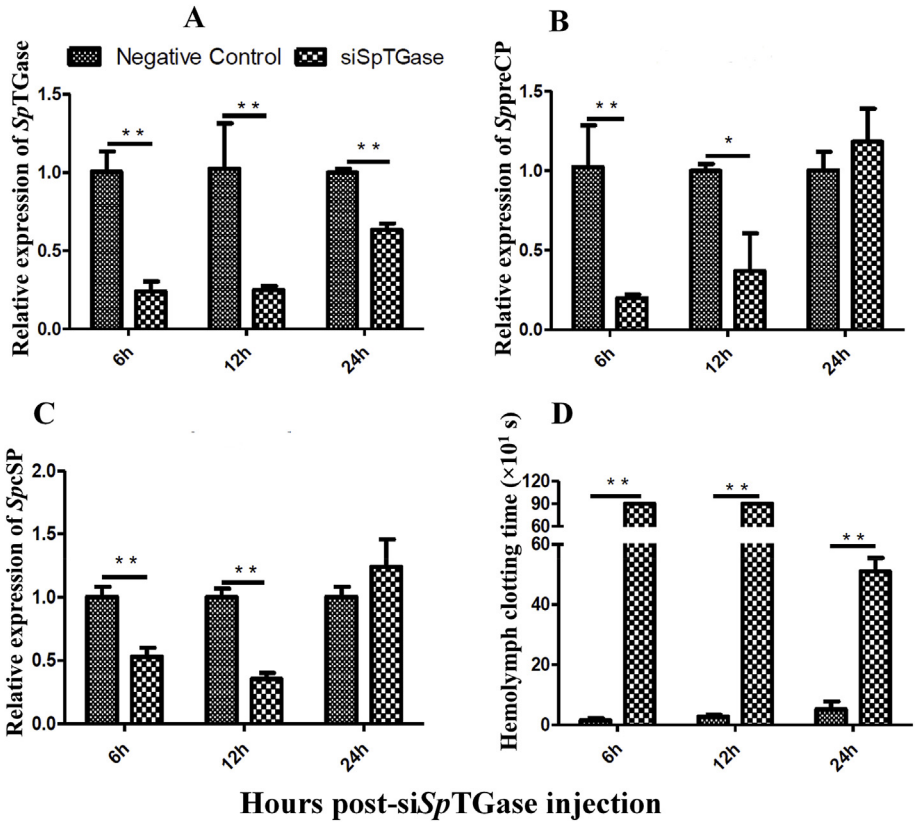

Fig. 8. Regulation of *Sp*TGase in the hemolymph clotting in mud crab. *Sp*TGase-siRNA modulated the expression of *Sp*TGase (A), *Sp*preCP (B) and *Spc*SP (C). Data were normalized to the β-actin. Each histogram represents the mean ± SE of three replicates. The hemolymph clotting time was observed in the hemolymph of mud crab at time points post-*Sp*TGase-siRNA injection (D). Data shown represent mean ± SE. Statistically significant differences from the control groups are marked as * $P < 0.05$ and ** $P < 0.01$.

ambiguous states were not found in *Sp*TGase (Fig. 4A). The search using SWISS-MODEL server revealed that the human transglutaminase 3 (PDB ID: 1l9m.1, Ahvazi, Kim [34]) at 2.1 Å resolution, showing 34.47% sequence identity, 39% similarity, and 87% query coverage (ranged from Val[55] to Glu[766] residues), was the best available template to build a 3-D model for *Sp*TGase protein. The similar template (PDB ID: 1l9mB, Ahvazi, Kim [34]) was also confirmed by COFACTOR and I-TASSER analyses. TM-scores (in COFACTOR) and normalized Z-score (in I-

TASSER) were 0.93 and 3.94, respectively, which indicated a good alignment between *Sp*TGase and its template. The predicted model for *Sp*TGase (at 1.5 Å resolution) and its structural analog were shown in Fig. 4B and C, respectively. A verification of the quality of the proposed model was conducted. Ramachandran plot analysis resulted in 85.7%, 12.3%, 1.2% and 0.8% of residues were found in the most favored, additional allowed, generously allowed and disallowed regions, respectively (Fig. S1A). The overall G-factor of the model was −0.17. The Lgscore and MaxSub values were −0.46 and −0.43, respectively. Z-Score value (ProSA analysis) was −7.47 and the plot of residue energies contained both positive and negative values (Fig. S1B and S1C). Results from ERRAT analysis showed 82.3 (< 95%) overall quality (Fig. S1D). Verify3D analysis revealed that 83.9% of the residues have averaged 3D-1D score ≥ 0.2 (Fig. S1E). PROVE analysis resulted in 0% buried outlier protein atoms in the predicted model.

Function prediction based on the structural similarity, performed by COFACTOR program, with human Transglutaminase 3 (PDB: 1nugA and 1nufA) revealed that the consensus prediction of GO terms suggested that *Sp*TGase is not only capable of transferase activity (GO:0016,740, $Cscore^{GO}$ = 0.96) and protein-glutamine gamma-glutamyltransferase activity (GO:0003810, $Cscore^{GO}$ = 0.95), but that it also exhibits calcium ion binding (GO:0005509, $Cscore^{GO}$ = 0.56) (Fig. S2A). Similarly, *Sp*TGase was found to bind to the Ca^{2+} ion (at Lys^{282}, Asn^{285}, Asn^{287}, Asp^{288}, and Asn^{291}) and Mg^{2+} ion (at Asp^{362}, Asp^{364}, Ser^{366}, and Thr^{368}) (both have a TM-score of 0.922) (Fig. 4D and E). Based on "biological process" prediction, the protein is a part of the cellular process (GO:0009987, $Cscore^{GO}$ = 0.91), single-organism process (GO:0044,699, $Cscore^{GO}$ = 0.83), and biological regulation (GO:0065,007, $Cscore^{GO}$ = 0.82) (Fig. S2B). Based on the term of "cellular component", it is predicted to act as intracellular part (GO:0044,424, $Cscore^{GO}$ = 1.00), organelle (GO:0043,226, $Cscore^{GO}$ = 0.91), and extracellular region part (GO:0044,421, $Cscore^{GO}$ = 0.82) (Fig. S2C).

3.3. Tissue distribution and expression profiles after infection

*Sp*TGase transcripts were found in all examined tissues (hepatopancreas, heart, gills, brain, muscles, intestine, skin and hemocytes). The highest expression was detected in hemocytes, while the lowest was in the heart (Fig. 5A). Changes in expression of *Sp*TGase in the hemocytes, skin, and hepatopancreas of mud crab after either *V. parahaemolyticus* or LPS or PolyI:C infection were observed at 0, 6, 12, 24, 48 and 96 hpi (Fig. 5B–D). In hemocytes, a significant increase in the levels of *Sp*TGase from 12 to 96 hpi with *V. parahaemolyticus* was found as compared to the controls. Expression of *Sp*TGase was found upregulated at 24 and 48 hpi, and finally downregulated (at 96 hpi) throughout the PolyI:C infection. Expression of *Sp*TGase following LSP challenge was significantly downregulated at 6, 12 and 12 h, and upregulated at 12 and 48 hpi. In skin, the expression level of *Sp*TGase was significantly downregulated at 6 and 12 hpi with *V. parahaemolyticus* which further gradually increased and reached a peak at 96 hpi, whereas kept increasing within 96 h after LPS or PolyI:C challenge. In hepatopancreas, a significant upregulation of *Sp*TGase was found at 6 and 12 h, 12 h, and 12 and 96 h after challenge with *V. parahaemolyticus*, LPS and PolyI:C, respectively, whereas a significant downregulation correspondingly observed at 24 and 96 h, 6 and 24 h, and 24 hpi.

3.4. Expression, purification and agglutinating activity

The polypeptide of about 53 kDa was observed in the lysate of *Rosetta* harboring the recombinant plasmid pGEX4T-1-*Sp*TGase, induced with IPTG, through SDS-PAGE analysis (Fig. 6A). The band size was accordant with the predicted molecular mass of the fusion protein. After a purification, the concentrations of r*Sp*TGase was determined as 87.5 μg mL^{-1}. The results of agglutination assay revealed the r*Sp*TGase capacity (at 3.6 μg mL^{-1}) of agglutination activities towards both Gram-negative bacteria (*V. alginolyticus*, *V. parahaemolyticus*, and *A. hydrophila*) and yeast (*S. cerevisiae*) (Fig. 6B). However, TBS-Ca^{2+} buffer, neither alone nor in combination with GST protein control was capable of agglutination activities on both Gram-negative bacteria and yeast. These results indicate that r*Sp*TGase can recognize molecules on the surface of both Gram-negative bacteria and yeast.

3.5. Interaction between SpTGase and SpcSP

To identify the interaction between r*Sp*TGase and r*Spc*SP, far-western blotting was employed. The results revealed that the bands were recognized by rabbit anti-r*Spc*SP antibody, while no bands observed in the GST control (Fig. 7), which indicates the direct binding capability between r*Sp*TGase and r*Spc*SP in the hemolymph of mud crab.

3.6. SpTGase silence influencing coagulation-related gene expression and hemolymph clotting time

The results of RNA interference revealed a significant decrease in transcripts of *Sp*TGase in *Sp*TGase siRNA-injected groups at 6 h post siRNA injection continuing over 24 h post siRNA injection and exhibited a maximal interference efficiency with 76% at 6 h as compared to the GFP-siRNA-injected control (Fig. 8A). RNA interference was used to confirm whether *Sp*TGase is involved in regulating the expression of coagulation-related genes, including *Sp*preCP and *Spc*SP. A significant downregulation in the expression of both *Sp*preCP and *Spc*SP genes was observed at 6 h and 12 h post siRNA injection, whereas no significant upregulation was observed at the later time point (24 h) (Fig. 8B and C). Regulation of hemolymph clotting by *Sp*TGase in mud crab was also investigated and the results showed that hemolymph clotting time in the *Sp*TGase siRNA-injected mud crab was longer than that in GFP-siRNA-injected control (Fig. 8D).

4. Discussions

Coagulation system is crucially important in animals, especially arthropods with an open circulatory system, for prevention of excess blood loss from a wound and keeping potential pathogens from entering the hemocoel [2,10]. In crustaceans, TGase is one of the crucial components of the hemolymph clotting system which has been reported to be located in the hemocytes and hematopoietic tissue [4,10]. TGase functions as a catalyze agent in order to generate the covalent crosslinks in proteins, participating in blood coagulation, skin barrier formation, extracellular-matrix assembly and other biological processes [35]. Recent studies have demonstrated that TGases participate in the immune response of crustacean species protecting the host against the pathogen invasion [4,9,10,13–15,36]. To date, TGases have been molecularly identified and functionally characterized in both invertebrates and vertebrates, showing high similarity with mammalian plasma factor XIIIa [13]. Nevertheless, the presence of TGase in mud crab remained unexplored so far.

In this study, mud crab *Sp*TGase comprised an ORF of 2304 bp encoding a putative protein of 767 amino acids. Physicochemical analyses indicated that *Sp*TGase was acidic (pI = 5.95), hydrophilic and highly soluble in water (GRAVY = -0.459), stable based on the instability index (II = 35.74) [37], and thermostable based on its aliphatic index (AI = 75.23) [38]. The comparison with orthologs in other crustaceans, such as crayfish (*P. leniusculus*) (including 766 aa) [10] and white shrimp (*L. vannamei*) (including 764 aa) [24], indicated an obtain of a complete sequence of *Sp*TGase. Neither a signal peptide nor a transmembrane domain was identified in the deduced amino acid sequence of *Sp*TGase, suggesting that *Sp*TGase was a typical cytoplasmic protein similar to that in tiger shrimp (*P. monodon*) [20], Chinese shrimp (*F. chinensis*) [22], white shrimp (*L. vannamei*) [23], and freshwater prawn (*M. rosenbergii*) [11]. Multiple sequence alignment

revealed that the presence of conserved RGD motif, TGc domain and catalytic sites (at Cys^{333}, His^{401} and Asp^{424}) in the protein sequence of *Sp*TGase with other TGases [10,11,20,22–24,39], indicating a high level of structural and functional conservation among the species of this protein. The RGD (Arg-Gly-Asp) and KGD (Lys-Gly-Asp) motifs are known as integrin binding sites [40], which plays roles in cell migration, extracellular matrix adhesion and cell to cell adhesion [41,42]. Herein, we found only one RGD motif in *Sp*TGase, but some TGases contained two RGD motif Arockiaraj, Gnanam [11], both of these (RGD and KGD) motifs Yeh, Tsai [24], or included only the KGD motif Zhu, Li [9]. The increased number of RGD motif refers the evolutionary pressures [11]. The result revealed that *Sp*TGase contained a main TGc domain, which shared similarity with those from other known crustaceans, such as *E. sinensis* [9], *P. vannamei* [24], *P. leniusculus* [10], *P. monodon* [21], suggesting its role was the same as that in other TGases. The previous studies [2,43] have shown that TG activity requires Ca^{2+}-binding leading to a modification in the proteins through acyl-transfer reactions. The function prediction based on the structural similarity showed that the residues Lys^{282}, Asn^{285}, Asn^{287}, Asp^{288}, and Asn^{291} were potential Ca^{2+}-binding sites in *Sp*TGase. The Ca^{2+}-binding sites in *Sp*TGase of mud crab are conserved except for one residue (Asn^{291}). The presence of catalytic sites along the main TGc domain also suggests the role in the TGase activity of *Sp*TGase, which is similar to other TGases reported previously from crustacean species [11,24].

Protein structure provides a better comprehension of the biological functions of a protein at the molecular level. The secondary structure of a protein is crucial for further folding and higher structural levels. In this study, we found that random coil was dominant in the secondary structure of *Sp*TGase, followed by extended strand, alpha helix and beta turn, which was similar with other available crustacean homologs, including *E. sinensis* (ADF87938.1), *L. vannamei* (ABX83902.1), *P. leniusculus* (AAK69205.1), *P. monodon* (AAV49005.1) (Table S1). This suggested a high similarity in the tertiary structure of this protein among these species. Overall 3-D structural analysis revealed that *Sp*TGase was similar to those of human TGase (PDB ID: 1l9m), indicating a high level of functional conservation of the protein. The 3-D proposed model was verified using many different tools. Verify3D analysis showed 83.9% ($> 80\%$) of the residues had averaged 3D-1D score ≥ 0.2, indicating a suitable model [44]. ERRAT analysis indicated a relatively low resolution of the structured model which only had 82.3 ($< 95\%$) overall quality [45]. Ramachandran plot analysis resulted in a total of 98% residues in the most favored and additional allowed regions [46]. The overall G-factor of the model showed the low quality of the model [28,30]. The discrepancy among the analysis maybe retrieved from the difference in applied methods among the tools and this is required to consolidate in further researches.

*Sp*TGase was widely expressed in all investigated tissues and the highest expression was observed in hemocytes, indicating that the *Sp*TGase was synthesized and stored in hemocytes, which secreted into the hemolymph, localized on the cell surface and extracellular matrix and attended to the blood clotting and immunoreactions after suffering an injury [2,3,9,11,20–24]. Furthermore, *Sp*TGase was observed to be mostly up regulated in the hemocytes, skin, and hepatopancreas of mud crab by various challenges, which suggested that TGase was involved in immune response in mud crab. Also, the results showed that r*Sp*TGase could produce agglutination on both Gram-negative bacteria (*V. alginolyticus*, *V. parahaemolyticus*, and *A. hydrophila*) and yeast (*S. cerevisiae*), suggesting that r*Sp*TGase was able to recognize the molecules located on the surface of both Gram-negative bacteria and yeast [33]. Recently, TGase has been confirmed to play an immunoregulation role in *L. vannamei* through the bacterial agglutinative activity against both *V. parahaemolyticus* and *Streptococcus iniae* [15]. The role of TGase in the immune response to microbes has been explained by the presence of functional domains (*N*-terminal domain, protease homologous domain, and Ig-like domain) in its structure. For instance, in *L. vannamei*, Ig-like domain (of LvTGase) showed the strongest agglutinative activity when compared to others [15]. In the present study, a similarity in structure between *Sp*TGase and LvTGase suggests that *Sp*TGase may have bactericidal activity *via* its containing domains. Further experiments, however, are required to confirm this preliminary speculation. Taken together, these results indicated that *Sp*TGase might be important in the immune system of mud crab for response to pathogen infections, similar to the data previously obtained in *L. vannamei* [15,23,24], *M. rosenbergii* [11], and *E. sinensis* [9].

Blood clotting system is known to be important in both invertebrates and vertebrates for prevention of excess blood loss from a wound and increase of the chances for survival through the obstructing the penetration of pathogens into the body cavity of the animal [4,10]. TGase has been reported to be involved in the rapid assembly of a plasma clotting protein [11]. In this study, we found that the silencing of *Sp*TGase led to the significantly decreased expression of both *Sp*preCP and *Sp*cSP genes, main components in crustacean hemolymph coagulation [14,33]. This data together with the longer blood clotting duration time after *Sp*TGase knockdown, partly because of the loss of coagulation activities of hemocytes in mud crab in our study.

In conclusion, *Sp*TGase was identified in mud crab in our study. Expression of *Sp*TGase was much higher in hemocyte compared with other tissues. r*Sp*TGase showed a capacity of agglutination activities towards both Gram-negative bacteria and yeast. *Sp*TGase gene silencing was positively correlated to the expression of both *Sp*preCP and *Sp*cSP genes and the longer duration time of the blood clotting, indicating its function in the hemolymph coagulation system in mud crab. However, further investigations are necessary to understand completely the mechanisms of *Sp*TGase in mud crab blood coagulation and immunity.

Acknowledgement

The work was supported by grants from National Natural Science Foundation of China (41876152, 31850410487, 31802341), China Postdoctoral Science Foundation (2018M643133), Guangdong provincial project of Science and Technology (2017B020204003), the “Sail Plan” Program for Outstanding Talents of Guangdong Province (14600605) and support from Department of Education of Guangdong Province (2017KCXTD014).

Appendix A. Supplementary data

Supplementary data related to this article can be found at https://doi.org/10.1016/j.fsi.2019.04.006.

References

[1] L. Vazquez, J. Alpuche, G. Maldonado, C. Agundis, A. Pereyra-Morales, E. Zenteno, Immunity mechanisms in crustaceans, Innate Immun. 15 (2009) 179–188.
[2] U. Theopold, O. Schmidt, K. Söderhäll, M.S. Dushay, Coagulation in arthropods: defence, wound closure and healing, Trends Immunol. 25 (2004) 289–294.
[3] T.G. Loof, O. Schmidt, H. Herwald, U. Theopold, Coagulation systems of invertebrates and vertebrates and their roles in innate immunity: the same side of two coins? J Innate Immun 3 (2011) 34–40.
[4] F.F. Fagutao, M.B.B. Maningas, H. Kondo, T. Aoki, I. Hirono, Transglutaminase regulates immune-related genes in shrimp, Fish Shellfish Immunol. 32 (2012) 711–715.
[5] M.-S. Yeh, Y.-L. Chen, I.-H. Tsai, The hemolymph clottable proteins of tiger shrimp, *Penaeus monodon*, and related species, Comp. Biochem. Physiol. B Biochem. Mol. Biol. 121 (1998) 169–176.
[6] L.M. Perazzolo, D.M. Lorenzini, S. Daffre, M.A. Barracco, Purification and partial characterization of the plasma clotting protein from the pink shrimp *Farfantepenaeus paulensis*, Comp. Biochem. Physiol. B Biochem. Mol. Biol. 142 (2005) 302–307.
[7] M.-S. Yeh, C.-J. Huang, J.-H. Cheng, I.-H. Tsai, Tissue-specific expression and regulation of the haemolymph clottable protein of tiger shrimp (*Penaeus monodon*), Fish Shellfish Immunol. 23 (2007) 272–279.
[8] M. Hall, R. Wang, R. van Antwerpen, L. Sottrup-Jensen, K. Söderhäll, The crayfish plasma clotting protein: a vitellogenin-related protein responsible for clot formation in crustacean blood, Proc. Natl. Acad. Sci. Unit. States Am. 96 (1999) 1965–1970.
[9] Y.-T. Zhu, D. Li, X. Zhang, X.-J. Li, W.-W. Li, Q. Wang, Role of transglutaminase in immune defense against bacterial pathogens via regulation of antimicrobial

peptides, Dev. Comp. Immunol. 55 (2016) 39–50.
[10] R. Wang, Z. Liang, M. Hall, K. Söderhäll, A transglutaminase involved in the coagulation system of the freshwater crayfish, *Pacifastacus leniusculus*. Tissue localisation and cDNA cloning, Fish Shellfish Immunol. 11 (2001) 623–637.
[11] J. Arockiaraj, A.J. Gnanam, R. Palanisamy, V. Kumaresan, P. Bhatt, M.K. Thirumalai, et al., A prawn transglutaminase: molecular characterization and biochemical properties, Biochimie 95 (2013) 2354–2364.
[12] G. Martin, J. Hose, S. Omori, C. Chong, T. Hoodbhoy, N. McKrell, Localization and roles of transglutaminase in hemolymph coahulation in decapods crustaceans, Comp. Biochem. Physiol. 3 (1991) 517–522.
[13] X. Lin, K. Söderhäll, I. Söderhäll, Transglutaminase activity in the hematopoietic tissue of a crustacean, *Pacifastacus leniusculus*, importance in hemocyte homeostasis, BMC Immunol. 9 (2008) 58.
[14] M.B.B. Maningas, H. Kondo, I. Hirono, T. Saito-Taki, T. Aoki, Essential function of transglutaminase and clotting protein in shrimp immunity, Mol. Immunol. 45 (2008) 1269–1275.
[15] Z. Zheng, W. Xu, J.J. Aweya, M. Zhong, S. Liu, J. Lun, et al., Functional domains of *Litopenaeus vannamei* transglutaminase and their involvement in immunoregulation in shrimp, Fish Shellfish Immunol. 81 (2018) 168–175.
[16] P.M. Steinert, S.-Y. Kim, S.-I. Chung, L.N. Marekov, The transglutaminase 1 enzyme is variably acylated by myristate and palmitate during differentiation in epidermal keratinocytes, J. Biol. Chem. 271 (1996) 26242–26250.
[17] S. Gambetti, A. Dondi, C. Cervellati, M. Squerzanti, F.S. Pansini, C.M. Bergamini, Interaction with heparin protects tissue transglutaminase against inactivation by heating and by proteolysis, Biochimie 87 (2005) 551–555.
[18] F. Tokunaga, T. Muta, S. Iwanaga, A. Ichinose, E.W. Davie, K.-i. Kuma, et al., Limulus hemocyte transglutaminase. cDNA cloning, amino acid sequence, and tissue localization, J. Biol. Chem. 268 (1993) 262–268.
[19] T. Osaki, N. Okino, F. Tokunaga, S. Iwanaga, S.-i. Kawabata, Proline-rich cell surface antigens of horseshoe crab hemocytes are substrates for protein cross-linking with a clotting protein coagulin, J. Biol. Chem. 277 (2002) 40084–40090.
[20] C.-C. Huang, K. Sritunyalucksana, K. Söderhäll, Y.-L. Song, Molecular cloning and characterization of tiger shrimp (*Penaeus monodon*) transglutaminase, Dev. Comp. Immunol. 28 (2004) 279–294.
[21] M.-Y. Chen, K.-Y. Hu, C.-C. Huang, Y.-L. Song, More than one type of transglutaminase in invertebrates? A second type of transglutaminase is involved in shrimp coagulation, Dev. Comp. Immunol. 29 (2005) 1003–1016.
[22] Y.-C. Liu, F.-H. Li, B. Wang, B. Dong, Q.-L. Zhang, W. Luan, et al., A transglutaminase from Chinese shrimp (Fenneropenaeus chinensis), full-length cDNA cloning, tissue localization and expression profile after challenge, Fish Shellfish Immunol. 22 (2007) 576–588.
[23] M.-S. Yeh, C.-H. Liu, C.-W. Hung, W. Cheng, cDNA cloning, identification, tissue localisation, and transcription profile of a transglutaminase from white shrimp, *Litopenaeus vannamei*, after infection by *Vibrio alginolyticus*, Fish Shellfish Immunol. 27 (2009) 748–756.
[24] M.-S. Yeh, W.-L. Tsai, W. Cheng, Identification and cloning of the second type transglutaminase from *Litopenaeus vannamei*, and its transcription following pathogen infection and in relation to the haemolymph coagulation, Fish Shellfish Immunol. 35 (2013) 1613–1623.
[25] K.C. Han-Ching Wang, C.-W. Tseng, H.-Y. Lin, I.T. Chen, Y.-H. Chen, Y.-M. Chen, et al., RNAi knock-down of the *Litopenaeus vannamei* Toll gene (*LvToll*) significantly increases mortality and reduces bacterial clearance after challenge with *Vibrio harveyi*, Dev. Comp. Immunol. 34 (2010) 49–58.
[26] Z. Sun, S. Hao, Y. Gong, M. Zhang, J.J. Aweya, N.T. Tran, et al., Dual oxidases participate in the regulation of hemolymph microbiota homeostasis in mud crab *Scylla paramamosain*, Dev. Comp. Immunol. 89 (2018) 111–121.
[27] Z. Wei, W. Sun, N.T. Tran, Y. Gong, H. Ma, H. Zheng, et al., Two novel serine proteases from *Scylla paramamosain* involved in the synthesis of anti-lipopolysaccharide factors and activation of prophenoloxidase system, Fish Shellfish Immunol. 84 (2019) 322–332.
[28] S. Cristobal, A. Zemla, D. Fischer, L. Rychlewski, A. Elofsson, A study of quality measures for protein threading models, BMC Bioinf. 2 (2001) 5.
[29] M.J. Sippl, Recognition of errors in three-dimensional structures of proteins, Proteins: Struct. Funct. Bioinf. 17 (1993) 355–362.
[30] M. Wiederstein, M.J. Sippl, ProSA-web: interactive web service for the recognition of errors in three-dimensional structures of proteins, Nucleic Acids Res. 35 (2007) W407–W410.
[31] K.J. Livak, T.D. Schmittgen, Analysis of relative gene expression data using real-time quantitative PCR and the $2^{-\Delta\Delta CT}$ method, Methods 25 (2001) 402–408.
[32] N. Okino, S.-i. Kawabata, T. Saito, M. Hirata, T. Takagi, S. Iwanaga, Purification, characterization, and cDNA cloning of a 27-kDa lectin (L10) from horseshoe crab hemocytes, J. Biol. Chem. 270 (1995) 31008–31015.
[33] D. Zhang, W. Wan, T. Kong, M. Zhang, J.J. Aweya, Y. Gong, et al., A clip domain serine protease regulates the expression of proPO and hemolymph clotting in mud crab, *Scylla paramamosain*, Fish Shellfish Immunol. 79 (2018) 52–64.
[34] B. Ahvazi, H.C. Kim, S.H. Kee, Z. Nemes, P.M. Steinert, Three-dimensional structure of the human transglutaminase 3 enzyme: binding of calcium ions changes structure for activation, EMBO J. 21 (2002) 2055–2067.
[35] L. Lorand, R.M. Graham, Transglutaminases: crosslinking enzymes with pleiotropic functions, Nat. Rev. Mol. Cell Biol. 4 (2003) 140.
[36] C.-C. Chang, H.-C. Chang, K.-F. Liu, W. Cheng, The known two types of transglutaminases regulate immune and stress responses in white shrimp, *Litopenaeus vannamei*, Dev. Comp. Immunol. 59 (2016) 164–176.
[37] K. Guruprasad, B.B. Reddy, M.W. Pandit, Correlation between stability of a protein and its dipeptide composition: a novel approach for predicting *in vivo* stability of a protein from its primary sequence, Protein Eng. Des. Sel. 4 (1990) 155–161.
[38] A. Ikai, Thermostability and aliphatic index of globular proteins, J. Biochem. 88 (1980) 1895–1898.
[39] J.M. Campbell, G.C. Fahey Jr., B.W. Wolf, Selected indigestible oligosaccharides affect large bowel mass, cecal and fecal short-chain fatty acids, pH and microflora in rats, J. Nutr. 127 (1997) 130–136.
[40] E. Ruoslahti, RGD and other recognition sequences for integrins, Annu. Rev. Cell Dev. Biol. 12 (1996) 697–715.
[41] S.S. Akimov, A.M. Belkin, Cell surface tissue transglutaminase is involved in adhesion and migration of monocytic cells on fibronectin, Blood 98 (2001) 1567–1576.
[42] A. Salsmann, E. Schaffner-Reckinger, F. Kabile, S. Plançon, N. Kieffer, A new functional role of the fibrinogen RGD motif as the molecular switch that selectively triggers integrin αIIbβ3-dependent RhoA activation during cell spreading, J. Biol. Chem. 280 (2005) 33610–33619.
[43] J. Kączkowski, Transglutaminase-an enzyme group of extended metabolic and application possibilities, Pol. J. Food Nutr. Sci. 14 (2005) 1.
[44] R. Lüthy, J.U. Bowie, D. Eisenberg, Assessment of protein models with three-dimensional profiles, Nature 356 (1992) 83.
[45] C. Colovos, T.O. Yeates, Verification of protein structures: patterns of nonbonded atomic interactions, Protein Sci. 2 (1993) 1511–1519.
[46] G.N. Ramachandran, C. Ramakrishnan, V. Sasisekharan, Stereochemistry of polypeptide chain configurations, J. Mol. Biol. 7 (1963) 95–99.